

1 **Intergenerational metabolic priming by sperm piRNAs**

2 Adelheid Lempradl^{1,2,*}, Unn Kugelberg^{3,†‡}, Mary Iconomou^{1,†‡}, Ian Beddows², Daniel Nätt³,
3 Eduard Casas⁴, Lovisa Örkenby³, Lennart Enders¹, Alejandro Gutierrez Martinez¹, Oleh
4 Lushchak⁵, Erica Boonen^{1,2}, Tamina Rückert¹, Martin Sabev¹, Marie G.L. Roth³, Dean Pettinga²,
5 Tanya Vavouri⁴, Anita Öst^{3,†*}, J. Andrew Pospisil^{1,2,†}

6 ¹ Max-Planck Institute for Immunobiology and Epigenetics, Stuebeweg 51, 79108 Freiburg,
7 Germany

8 ² Van Andel Research Institute, 330 Bostwick Ave. N.E., MI 49503, USA, current address for
9 AL and JAP

10 ³ Department of Biomedical and Clinical Sciences, Linkoping University, 581 83 Linkoping,
11 Sweden

12 ⁴ Josep Carreras Leukaemia Research Institute (IJC), Campus ICO-IGTP-UAB, Ctra. de Can
13 Ruti, Camí de les Escoles s/n, 08916 Badalona, Barcelona, Spain

14 ⁵ Vasyl Stefanyk Precarpathian National University, 57 Shevchenko Str., Ivano-Frankivsk,
15 76018, Ukraine

16 [†] These authors contributed equally

17 [‡] These authors contributed equally

18 * Correspondence to: anita.ost@liu.se and heidi.lempradl@vai.org

20 **Summary:** Preconception parental environment can reproducibly program offspring phenotype
21 without altering the DNA sequence, yet the mechanisms underpinning this ‘epigenetic inheritance’
22 remains elusive. Here, we demonstrate the existence of an intact piRNA-pathway in mature
23 *Drosophila* sperm and show that pathway modulation alters offspring gene transcription in a
24 sequence-specific manner. We map a dynamic small RNA content in developing sperm and find
25 that the mature sperm carry a highly distinct small RNA cargo. By biochemical pulldown, we
26 identify a small RNA subset bound directly to piwi protein. And, we show that piRNA-pathway
27 controlled sperm small RNAs are linked to target gene repression in offspring. Critically, we find
28 that full piRNA-pathway dosage is necessary for the intergenerational metabolic and
29 transcriptional reprogramming events triggered by high paternal dietary sugar. These data provide
30 a direct link between regulation of endogenous mature sperm small RNAs and transcriptional
31 programming of complementary sequences in offspring. Thus, we identify a novel mediator of
32 paternal intergenerational epigenetic inheritance.

33

34 **Introduction**

35 Current data suggest obesity as one of the world's chief socioeconomic challenges of our day,
36 impacting ~1 billion individuals worldwide. The dramatic rise in metabolic disease incidence in
37 the last decades, particularly in children, suggests a prominent role for epigenetic mechanisms, in
38 particular, a role for intergenerational epigenetic mechanisms where physiological effects in
39 parents (e.g. diet, hyperglycemia, obesity) trigger disease-predisposing shifts in the offspring
40 through non-DNA-sequence-based mechanisms. To date, the mechanisms mediating
41 intergenerational epigenetic programming in response to physiological state remain poorly
42 understood.

43

44 PIWI-interacting RNAs (piRNAs) are 24-32 nucleotide, PIWI-bound small RNAs that are best
45 known for silencing transposable elements and thereby limiting their mutagenic potential¹⁻³. This
46 canonical function of piRNAs is essential for germline genome integrity and is active in most
47 animals⁴. The piRNA-pathway differs from other small RNA (sRNA) pathways (miRNA, siRNA)
48 in three key aspects: 1) piRNA-pathway protein expression is mainly restricted to reproductive
49 organs; 2) piRNAs are generated through a Dicer-independent mechanism; and 3) piRNAs are
50 processed from single stranded precursor transcripts, making mRNAs theoretical sources and
51 substrates for piRNA generation and amplification.

52

53 Canonical piRNAs are derived from genome regions called piRNA clusters, which harbor ancient
54 transposon fragments. Accumulating evidence in both flies and mice suggests that piRNAs can
55 also be produced from genic mRNAs⁵⁻¹⁰. In male mice, about 20% of the piRNA population in
56 pre-pachytene germ cells for example, is derived from the exons of hundreds of mRNAs⁵. piRNAs
57 derived from 3'UTRs have also been found in follicle cells of fly ovaries and *Xenopus* eggs^{6,7,10}.
58 Although piRNAs were first identified in *Drosophila* testis¹¹, much of the pioneering work in flies
59 has focused on the female germline¹². In general, the sRNA content of the male *Drosophila*
60 germline is ill characterized. Specifically, piRNA populations, their dynamics during
61 spermatogenesis and their potential functional roles, remain poorly understood.

62

63 In *C. elegans*, piRNAs have been implicated in the multigenerational inheritance of foreign DNA-
64 triggered epigenetic silencing¹³. In these contexts, once piRNA-seeded silencing states are initially

65 established, their long-term memory is independent of the original piRNA trigger, and instead
66 relies on nuclear RNAi and chromatin pathways. Notable, maternal piRNAs have been shown to
67 buffer against DNA sequence incompatibility between maternal and paternal genomes, in
68 particular at transposons, a phenomenon known as hybrid dysgenesis¹⁴. Here, we identify an intact
69 mature sperm piRNA pathway and provide evidence for its involvement in both encoding and
70 decoding intergenerational inheritance effects.

71

72 **Dynamic sRNA expression in the male *Drosophila* germline**

73 The tube-shaped *Drosophila* testis has contributed significantly to our understanding of stem cell
74 maintenance and germ cell differentiation¹⁵. To understand the dynamics of sRNA populations
75 during spermatogenesis we performed sRNA sequencing on testes manually dissected into four
76 parts: 1) testis tip (T1) containing stem cells and primary spermatocytes, 2) the apical portion (T2)
77 containing meiotic and developing spermatogonia, 3) the distal portion (T3) containing late-stage
78 spermatocytes undergoing individualization, and 4) mature sperm (Sperm) isolated from seminal
79 vesicles (Fig. 1A-C). Principal component analysis revealed high technical reproducibility.
80 Interestingly, the greatest variation (PC1) separated sperm from testis samples; PC2 separated the
81 three stages of testis development (Fig. 1B). These data indicate that the mature sperm sRNA
82 repertoire is highly distinct from that of the developing germ cells. Relative to T1-T3, sperm
83 showed an *increase* in sRNAs mapping to protein coding genes (3' UTRs and exons) and tRNAs,
84 and a *decrease* in repeat-associated sRNAs (piRNA clusters, complex and simple repeats) (Fig.
85 1C). These results resemble findings in the male mouse germline, where a loss of piRNAs and a
86 gain of tRNA and mRNA fragments was shown for the transition from testicular to caput sperm¹⁶.
87 Sperm sRNAs mapping to protein coding exons exhibited a high correlation with sperm mRNA-
88 seq datasets ($r=0.92$, $p<0.0001$; Fig. 1D), consistent with the mRNA degradation that occurs in
89 late spermatogenesis. Fly and human sperm¹⁷ sRNA (Fig. 1E and F) repertoires showed critical
90 similarity at the biotype level, sharing for instance seven of the ten most highly expressed tRNA
91 genes (Fig. 1G), thus highlighting the evolutionary conservation. These results comprise the first
92 in-depth analysis of sRNA dynamics in *Drosophila* spermatogenesis; they demonstrate a highly
93 specific sperm sRNA population relative to the developing germline; and, they show conservation
94 in sRNA composition between *Drosophila* and mammals.

95

96 **Evidence for a functional piRNA-pathway in mature sperm**

97 One key outstanding question about sperm sRNAs in the context of intergenerational control is
98 how the minimal RNA load of a single sperm cell can reprogram the developmental trajectory of
99 a whole organism. The amplification mechanism of the piRNA-pathway provides one possibility
100 by which quantal differences in sRNAs might trigger reproducible next-generation effects as well
101 as a range of penetrance distributions. piRNAs were originally identified and characterized based
102 on their direct binding to PIWI proteins ¹⁸⁻²². If piRNAs were involved in epigenetic inheritance,
103 we reasoned that they would be loaded onto the appropriate protein machinery in mature sperm.
104 Previous work showed that Piwi protein is stably expressed in somatic and early germ-cells in the
105 apical testis ²³. Consistent with those reports, we found Piwi immunoreactivity in the nuclei of
106 multiple germline and somatic cell types in the tip of the testis (Supplemental Fig. 1A).
107 Interestingly, we also found piwi protein in individualizing, late stage spermatids at the distal end
108 of the testis, and in washed and purified sperm isolated from the sperm sack when using anti-Piwi
109 antibody raised against a peptide from the middle of the protein (Fig. 2A left; see Materials and
110 Methods for antibody details;). Piwi immunoreactivity appeared both as puncta along the sperm
111 tail (Fig. 2A center) and as a highly reproducible single body at the base of each compacted sperm
112 nucleus (Fig. 2A right, and secondary antibody control in Supplemental Fig. 1B). This result is in
113 agreement with results from mouse showing PiwiL1 protein presence in mature sperm²⁴. Western
114 blots confirmed our result by detecting the full-length Piwi protein in isolated sperm and ovaries
115 (~97 kDa; Western blot, Fig. 2B left and middle panel). Samples containing empty seminal
116 vesicles showed no evidence of Piwi protein, which argues against possible contribution of somatic
117 cell contamination to the signal in sperm. Further, we isolated protein lysates from ovaries, testis,
118 and purified sperm of flies carrying a BAC Piwi-GFP transgene. In contrast to wild-type, Western
119 blot of Piwi-GFP transgenic sperm revealed two bands, matching the sizes of GFP-tagged and
120 wild-type Piwi protein (Fig. 2C). Thus, both wild-type and transgenic Piwi protein are found in
121 sperm, confirming the specificity of the antibody.

122

123 Seeking to leverage an antibody-independent technique, we performed targeted mass spectrometry
124 on protein extracts of purified sperm (Supplemental Fig. 1C). For Piwi, we found signals for all
125 possible targetable Piwi peptides after tryptic digestion. Importantly, peptides were also detected
126 for the remaining two PIWI proteins known to be necessary for amplification of silencing

127 competent piRNAs, namely aubergine (Aub) and argonaute 3 (AGO3)(Supplemental Fig. 1C).
128 Thus, intact PIWI pathway proteins are consistently expressed in mature sperm and may therefore
129 serve as facilitators of intergenerational inheritance of functional piRNAs.

130
131 To identify piwi-associated sRNAs we used the sperm specific Piwi antibody to develop and
132 optimize a biochemical pulldown and sequencing approach (Piwi-RIP-seq) applicable to the
133 minute amounts of Piwi protein and RNA available in dissected *Drosophila* sperm. After rounds
134 of protocol optimization, we profiled the Piwi-bound sRNA content in sperm from 4 replicates
135 each of ~750 hand-dissected seminal vesicles (Piwi-RIP-seq). Piwi-pulldown enriched sRNAs
136 showed a peak length of ~25nt (Fig. 2D left) and an A-bias at the first nucleotide position (Fig. 2D
137 right), consistent with published data from ovaries¹⁸. Using a stringent mapping and hierarchical
138 annotation approach and rRNA exclusion (see methods), we found enrichment for sRNAs from
139 piRNA clusters, repeats and transposons, and to a lesser extent those from protein coding exons,
140 5'UTRs and ncRNAs (Fig. 2F, top). By contrast, sRNAs *not* associated with piwi protein in the
141 pull-down experiment showed a peak length of ~21-23 nt (Fig. 2E) and were enriched for miRNAs,
142 tRNAs, snRNAs, snoRNAs pseudogenes and 3'UTRs (Fig. 2F, bottom). Importantly, Piwi-bound
143 RNAs exhibited an anti-correlation with total sRNA content of sperm (Fig. 2G). These data
144 indicated highly specific loading of sRNAs onto Piwi and also argued against non-specific
145 pulldown effects in the Piwi-RIP-seq results. Pathway analysis of protein coding exon-derived
146 sRNAs showed enrichments for genes involved in phosphorylation, metabolism, gametogenesis,
147 development and cilium organization (Fig. 2I). To test for potential chromatin state associated
148 enrichment we next mapped our Piwi-RIP-seq dataset to published *Drosophila* chromatin state
149 annotations derived from genome-wide binding analysis of over 50 functional chromatin-binding
150 proteins²⁵. Interestingly, this intersection showed a striking enrichment for sRNAs from transcripts
151 that map to chromatin states with clear repressive signatures. These enriched states were described
152 as Lamin / H1-associated, “Black” chromatin and Polycomb-associated, “Blue” chromatin in
153 embryonic cells (Fig. 2H and Fig S1 D). Thus, mature sperm harbors a highly specific complement
154 of Piwi-bound sRNAs (piRNAs).

155
156 **Piwi controlled sperm RNAs regulate offspring gene transcription**

157 Working from the hypothesis that sperm piRNAs might regulate offspring transcription, we
158 examined the effect of *parental* heterozygous *aub* mutation (*aub*^{*Het*}) on next-generation
159 transcriptional output (embryos, stage 17). Aub participates in the ping-pong cycle of the PIWI
160 pathway and is necessary for amplification of silencing competent piRNAs and robust gene
161 repression^{26,27}. We compared mRNA transcriptional changes elicited in offspring from two parallel
162 mutant crosses (Fig. 3A and B): *aub*^{*Het*} mothers x WT fathers (maternal *aub*^{*Het*} offspring); and WT
163 mothers x *aub*^{*Het*} fathers (paternal *aub*^{*Het*} offspring)(data expressed relative to wildtype offspring
164 from parallel WT x WT crosses; WT offspring). In order to ensure comparable genetic
165 backgrounds, we prepared for the experiment by backcrossing *aub*^{*Het*} flies to our own highly inbred
166 w1118 background (WT) (see supplemental methods for details). The mRNA transcriptional
167 response in maternal *aub*^{*Het*} offspring revealed a strong correlation with our RIP-seq defined sperm
168 piRNAs (Fig. 3C), specifically, derepression of piRNA-sequence matching ‘targets’. These data
169 suggested that wild-type Piwi-bound sperm RNAs directly or indirectly trigger silencing of
170 sequence-matching loci in the next-generation (zygote). This conclusion agrees with previous
171 findings that maternal depletion of Piwi impacts heterochromatin formation in the offspring²⁸. In
172 reciprocal crosses, the paternal *aub*^{*Het*} mutation failed to trigger a similar piRNA dependent
173 offspring transcriptional response (Fig. 3D) indicating a parent-of-origin directionality to the
174 system. Thus, offspring transcription is modulated in a parent-specific manner by piRNA-pathway
175 dosage.

176
177 To gain further insights into the nature of parent-specific transcriptional changes in offspring, we
178 compared the changes triggered in maternal-*aub*^{*Het*} offspring to those of paternal-*aub*^{*Het*} offspring,
179 and identified three classes of intergenerationally-responsive transcripts and associated sRNAs:
180 **Class I** transcripts (Fig. 3B **Purple**; n=1046) were upregulated in offspring of both maternal and
181 paternal *aub*^{*Het*} crosses ($\text{Log}_2\text{FC} > 0.5$). Class I transcript sequence matching sRNAs were enriched
182 in our Piwi-RIP-seq indicating these transcripts are ‘targets’ of bona fide Piwi-bound sperm
183 piRNAs (Fig. 3F). Class I transcripts were enriched for transposons (Supplemental Fig. 2A) which
184 is in agreement with the canonical role of piRNAs in transposon silencing. Together, these data
185 indicate that Class I genes in the embryo are targets of paternal piRNAs and their repression in the
186 offspring requires zygotic aub activity. They identify a novel intergenerational sequence-specific
187 gene regulatory axis.

188 **Class II** transcripts (n=494), by contrast, were upregulated *only* in offspring of paternal *aub*^{*Het*}
189 crosses (Fig. 3B, **Green**; paternal Log₂FC > 0.5; maternal Log₂FC < -0.5). sRNAs mapping to
190 Class II transcripts were depleted in the Piwi-IP (Fig. 3E) and, interestingly, were highly and
191 specifically expressed in sperm (Fig. 3G). Further experiments revealed that sRNAs mapping to
192 Class II transcripts were sensitive to both *aub* and *piwi* dosage in the male germline (reduced
193 expression in *aub*^{*Het*} (Fig. 3E) and in *piwi*^{*Het*} (Supplemental Fig. 2B) sperm sRNAseq). These data
194 identify a novel subclass of highly expressed sRNAs in sperm whose abundance is sensitive to *aub*
195 and *piwi* dosage. Thus, Class II genes are intergenerationally regulated transcripts responsive to
196 paternally inherited, piRNA-pathway sensitive sRNAs.

197 **Class III** transcripts (n=1036) were down regulated in offspring of both maternal and paternal
198 *aub*^{*Het*} crosses (Fig. 3B, **Dark Grey**; Log₂FC < -0.5). The Class III genes had no detectable
199 signatures associated with transposon content (Supplemental Fig. 2A), Piwi-binding (Fig. 3F), or
200 piRNA-pathway sensitivity (Fig. 3E and Supplemental Fig. 2B). There were only 20 **Class IV**
201 transcripts that were specifically upregulated in maternal crosses (and only six with sequence-
202 matching sperm sRNA reads, Fig. 3B, **Light Grey**; paternal Log₂FC < -0.5; maternal Log₂FC >
203 0.5). Importantly, to rule out potentially confounding influences of the arbitrary expression change
204 cutoffs used above we repeated the analysis using a threshold free stratified *Rank-Rank*
205 *Hypergeometric Overrepresentation* (RRHO) approach ²⁹(Right side of Fig. S2). RRHO validated
206 the interpretations above and the existence of Class I, II, and III transcripts (Fig. S2C) and their
207 associated sRNA signatures (Fig. S2 D-F).

208
209 Gene set over-representation analysis showed enrichment in signaling and neuronal pathways (Fig.
210 S2G top) for Class I (purple) genes. Class II (green) genes were enriched for metabolic, hydrolase
211 activity and neuronal pathways (Fig. S2 middle), and Class III genes (dark gray) were enriched for
212 cell cycle pathways (Fig. S2G bottom) genes. Consistent with the enrichments observed in our
213 sperm Piwi-RIP-seq data (Fig. 3F), Class I genes were mostly positioned in “Black” Lamin / H1-
214 and “Blue” Polycomb-associated repressive chromatin annotations (Fig. 3H, Class I).
215 Interestingly, while not enriched in the IP, Class II genes also showed similar chromatin state
216 association (Fig. 3H, Class II). Both of these annotations have been suggested to include
217 enrichments for developmentally naive chromatin compartments and the data are therefore
218 coherent with a mechanism for modulation of early embryo development. No such enrichment was

219 found for Class III genes (Fig. 3H, Class III). These data are consistent with a mechanism whereby
220 Class I and Class II *sRNAs* promote targeted, chromatin state specific silencing of offspring gene
221 transcription. Thus, *paternal Piwi-bound sRNAs* and *paternal PIWI-sensitive sRNAs*, respectively,
222 are necessary for next-generation repression of Class I & II genes.

223

224 **The piRNA-pathway is required for paternal inheritance of metabolic state**

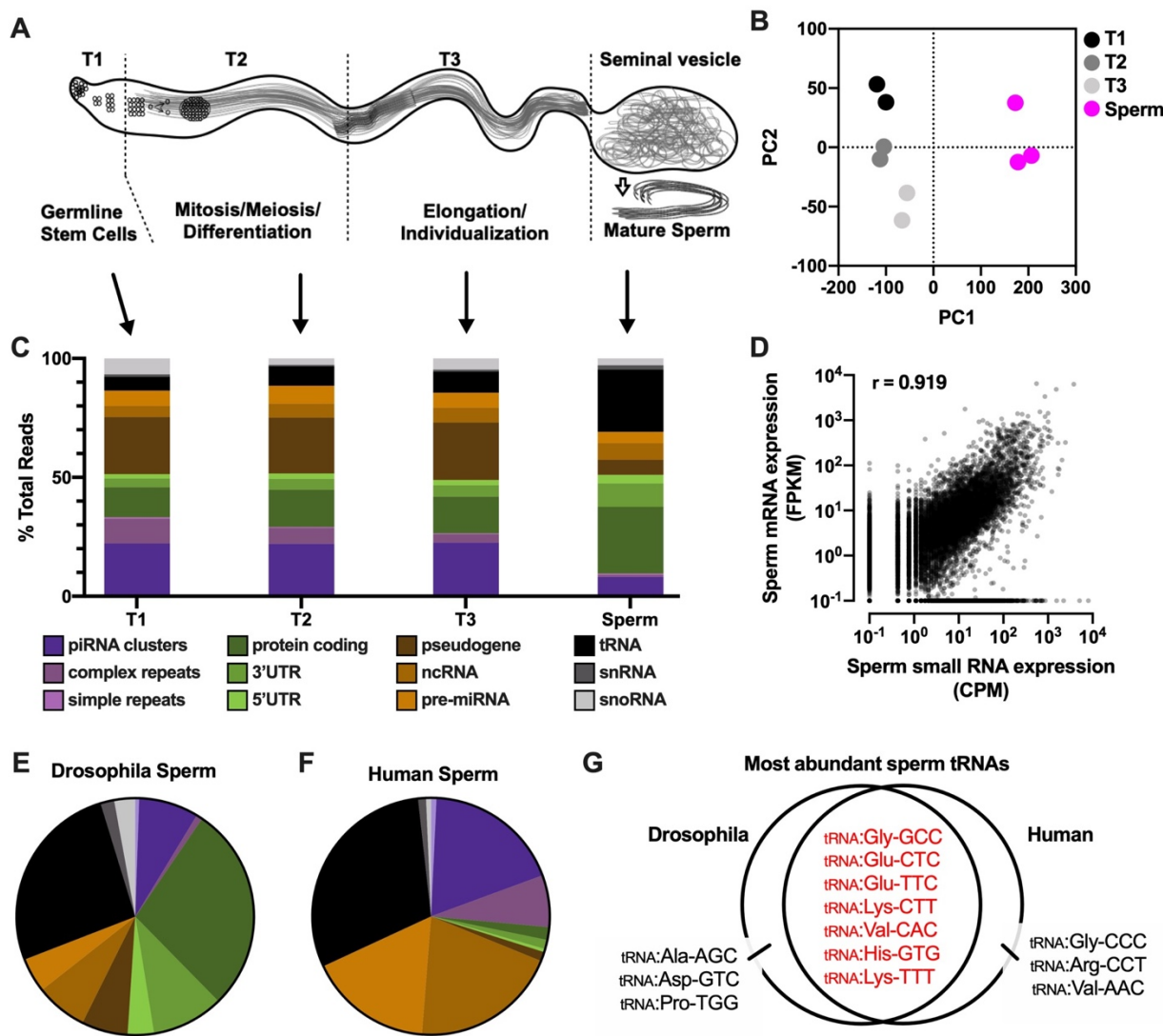
225 We previously identified similar chromatin-state and metabolic pathway signatures in offspring of
226 a paternal diet-induced model of *InterGenerational Metabolic Reprogramming* (IGMR)³⁰. In that
227 model (depicted in Fig. 4A), a two-day dietary sugar intervention in fathers before mating leads to
228 obesity in adult offspring (~10% increase in adult fat content), and in embryos, to transcriptional
229 changes reminiscent of chromatin silencer deficiency. Guided by the similarities we tested for
230 evidence of piRNA-pathway dependency in IGMR. We compared expression of the different
231 Classes identified above (Fig. 3) to datasets from IGMR offspring. Intriguingly, while Class I
232 genes showed no evidence of regulation in IGMR, Class II (piRNA-pathway dosage sensitive)
233 genes showed significant upregulation in offspring of high sugar fed fathers (green; Fig. 4B),
234 including strong enrichment of the most upregulated IGMR genes (upper bulge in the green violin;
235 rank analysis, Fig. 4C). Embryonic transcription of Class II genes is thus sensitive to paternal
236 dietary sugar; from a different point-of-view, diet-triggered intergenerational responses mimic
237 those induced by *aub* and *piwi* heterozygosity in the male germline (paternal-*aub*^{*Het*} and -*piwi*^{*Het*}).
238 Signed rank correlation (Fig. 4D) and RRHO (Fig. S3A) analysis validated these findings genome-
239 wide. Comparing IGMR and maternal-*aub*^{*Het*}-induced intergenerational responses did not show
240 the same trend (Fig. 4D and S3B). The converse analysis, examining the most up- and down-
241 regulated IGMR genes, confirmed these findings: Genes most upregulated in high sugar sired
242 embryos showed the same signatures as Class II genes described above: they were upregulated in
243 paternal, but downregulated in maternal *aub*^{*Het*} crosses (Fig S3C), and sRNAs mapping to these
244 genes were downregulated in *aub*^{*Het*} mutant sperm and depleted from the Piwi pulldown (Fig S3D).
245 Thus, paternal dietary sugar and piRNA-pathway deficiency trigger comparable intergenerational
246 transcriptional rewiring in offspring. This indicates that IGMR is dependent on the dosage of sperm
247 piRNA-pathway-regulated sRNAs.
248 If these piRNA sensitive genesets were causal with respect to intergenerational reprogramming,
249 we reasoned that piRNA-pathway mutant fathers should fail to trigger an IGMR response. To this

250 end, we tested whether piRNA-pathway heterozygote fathers (*piwi*^{*Het*} and *aub*^{*Het*}) were capable of
251 eliciting a full IGMR obesity response using our previously published intergenerational dietary
252 model. We performed the intergenerational diet experiment using WT and *piwi*^{*Het*} and *aub*^{*Het*}
253 fathers. Despite normal fertility and reproductive function in *piwi*^{*Het*} and *aub*^{*Het*} fathers, we found
254 that both heterozygote lines failed to elicit increased triglyceride accumulation in the next
255 generation (Fig. 4F). Thus, full piRNA-pathway dosage is necessary for paternal diet-induced
256 intergenerational obesity (IGMR).

257

258 In summary, we describe a highly dynamic sRNA repertoire during *Drosophila* spermatogenesis.
259 We find that sperm contains full-length piRNA-pathway proteins, and, using pulldown
260 approaches, prove the existence of Piwi-bound piRNAs in sperm. Heterozygous mutations in
261 piRNA-pathway member proteins lead to changes in sperm sRNAs indicating that mild pathway
262 disruption is sufficient to alter the sperm sRNA load transferred to the zygote *and* to alter
263 transcription in the next generation early life. Significant correlation between paternal Piwi bound
264 (Class I) and Piwi sensitive (Class II) sRNAs and offspring gene transcription indicates that
265 paternal sRNAs are involved in intergenerational inheritance by targeting sequence-matched genes
266 for silencing in the next generation. Indeed, using paternal sugar triggered IGMR as a test case,
267 we confirm this hypothesis and provide genetic evidence that a fully intact piRNA-pathway is
268 necessary for intergenerational inheritance of paternal metabolic state (Summarized in Fig. 4G).

269 **Fig. 1:**

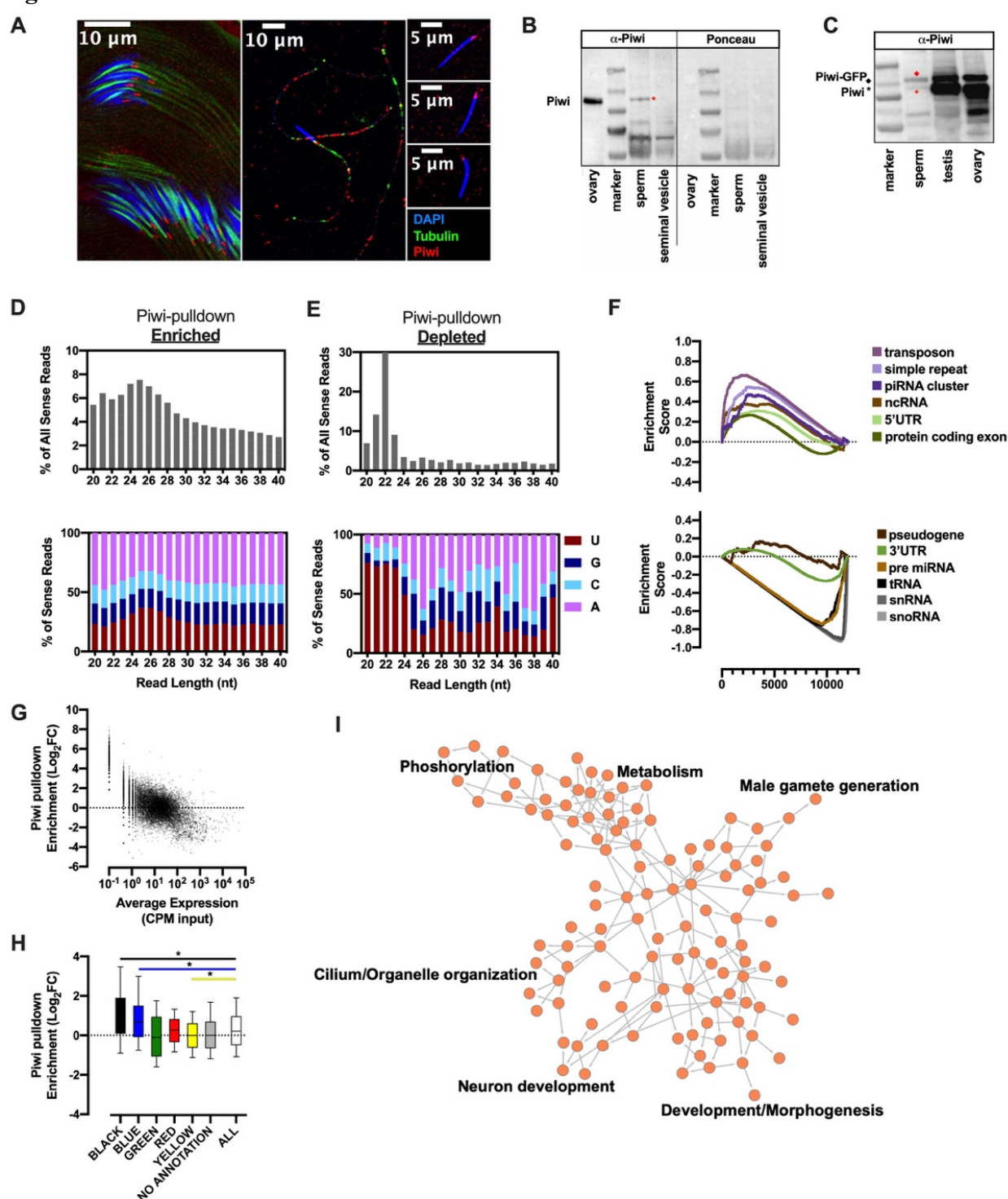


270

271 **Fig. 1: Dynamic sRNA expression in the male *Drosophila* germline**

272 A schematic of the *Drosophila* testis indicating segments used for sRNA sequencing; B) PCA
273 plot of sRNA sequencing data; C) % read distribution across biotypes and across testis segments;
274 biotype color legend applies to panels C, E and F; D) correlation of sRNA sequencing results with
275 previously published mRNA sequencing³⁰ results from mature sperm and showing Pearson's r; E)
276 *Drosophila* sperm and F) human sperm sRNA biotype distributions; G) 10 most enriched tRNA
277 features in *Drosophila* and human sperm¹⁷ sRNA sequencing.
278

279 **Fig. 2:**

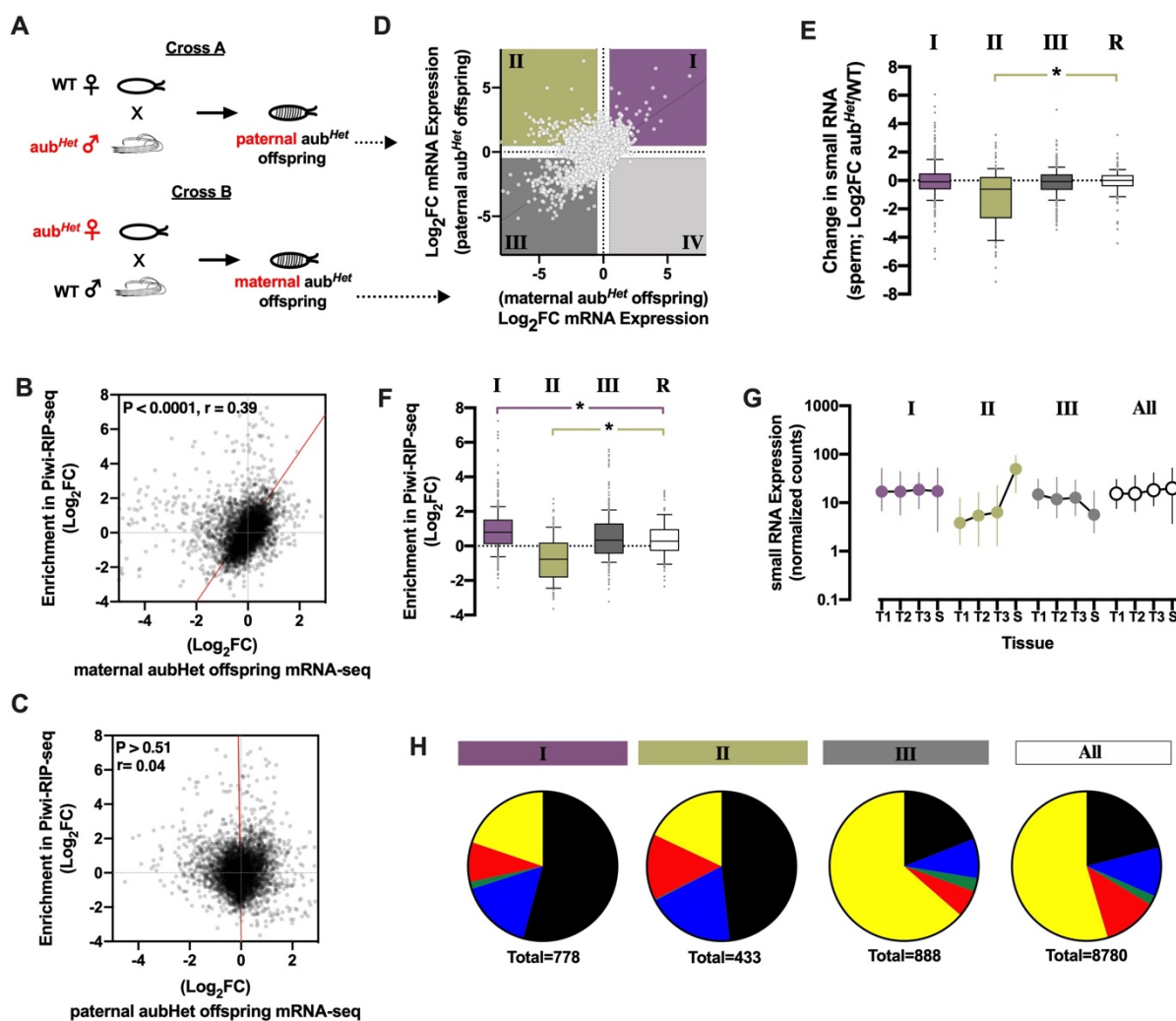


280
281
282
283
284
285

Fig. 2: Presence of Piwi bound RNAs in mature *Drosophila* sperm A) immunofluorescence staining of sperm with Piwi (ab5207) and tubulin antibodies; B) left panel shows western blot with Piwi antibody (ab5207) for ovary, sperm and empty seminal vesicle, right panel shows Ponceau staining to show protein content per lane. C) sperm, testis and ovaries from GFP-Piwi flies, the upper band shows the GFP fusion protein, lower band shows WT Piwi; D-E) length distribution

286 (left) and 1st nucleotide bias (right) of sense reads mapping to all features displayed as percentages
287 of all reads between the length of 20-50nt for significantly enriched (D) and for significantly
288 depleted features in Piwi-IP (piwi-antibody ab5207)(E); F) GSEA analysis of sRNA results using
289 custom pathways for the individual biotypes used for annotation; G) average counts per million
290 (CPM) in input samples versus Log₂FC in Piwi pulldown samples H) enrichment of reads mapping
291 to features embedded in different chromatin states. I) Pathway overrepresentation analysis
292 (WebGestalt)³¹ of protein coding features significantly enriched in Piwi pulldown.

293 **Fig.3:**



294

Fig. 3: Paternal piRNAs reprogram offspring

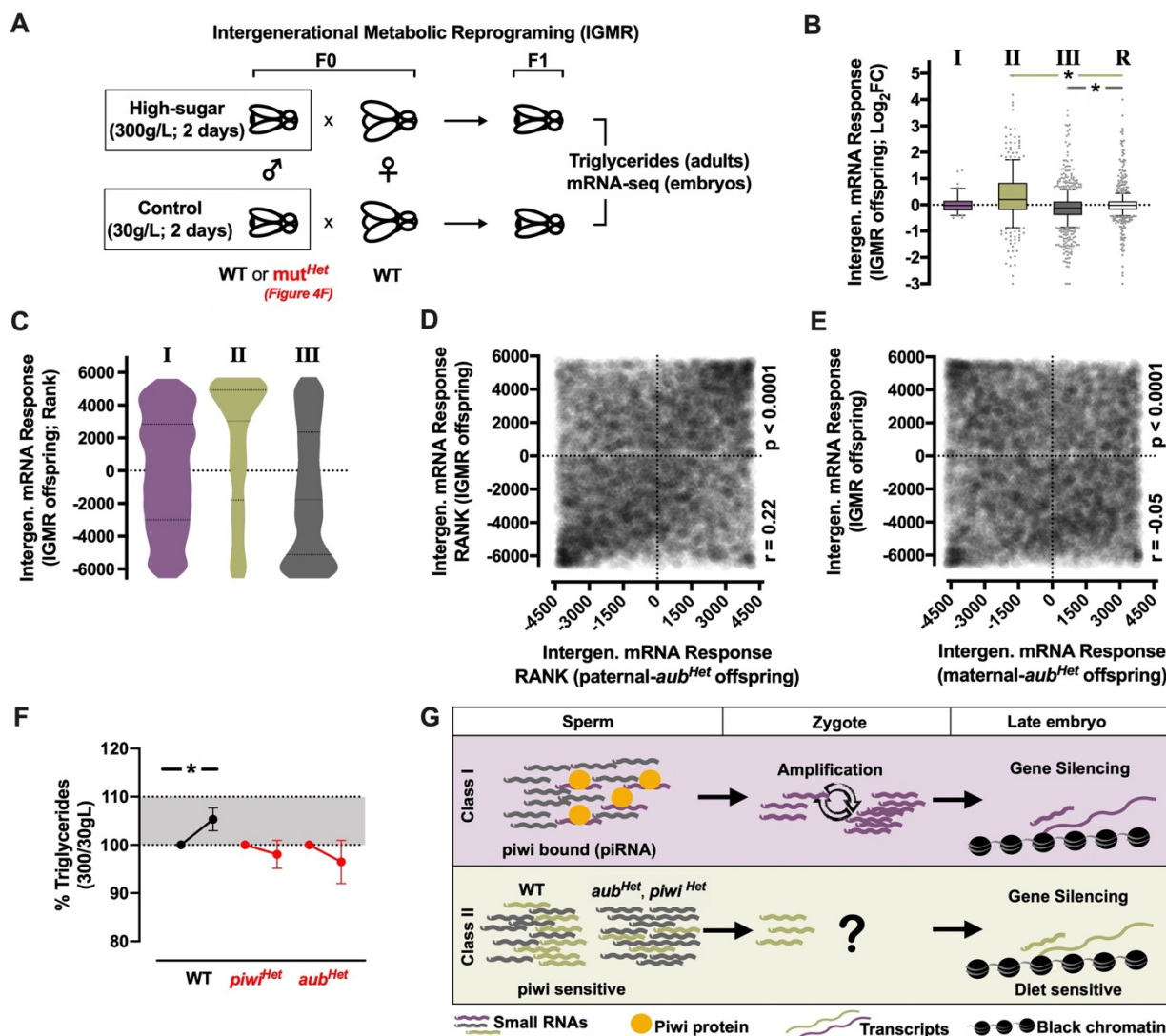
295 A) crossing scheme; B) comparison of mRNA expression changes induced by paternal vs
296 maternal aub^{Het}, coloring and numbering is kept consistent throughout manuscript; C) correlation
297 between Piwi pulldown enrichment and mRNA expression changes in maternal aub^{Het} offspring;
298 D) correlation between Piwi pulldown enrichment and mRNA expression changes in paternal
299 aub^{Het} offspring; E) Log₂FC of sperm sRNAs in aub^{Het} vs WT males, each boxplot represents
300 genes present in a different quadrants (Class) in D, random gene set in white F) Enrichment
301 (Log₂FC IP/Input) of sequence matching sRNAs in Piwi pulldown (Piwi-RIP-seq), each boxplot
302 represents sequences matching genes present in a different quadrant (Class/color) from E; G)
303 normalized counts in sRNA testis samples (as shown in Fig. 1) mapping to features in different
304 quadrants in D, all genes in white; H) chromatin state annotations of Class I-III genes compared
305 to all genes (right). Paternal aub^{Het} offspring n=5, WT offspring n=5, maternal aub^{Het} offspring
306 n=2 with each replicate containing a pool of 20 embryos.

307

308

309

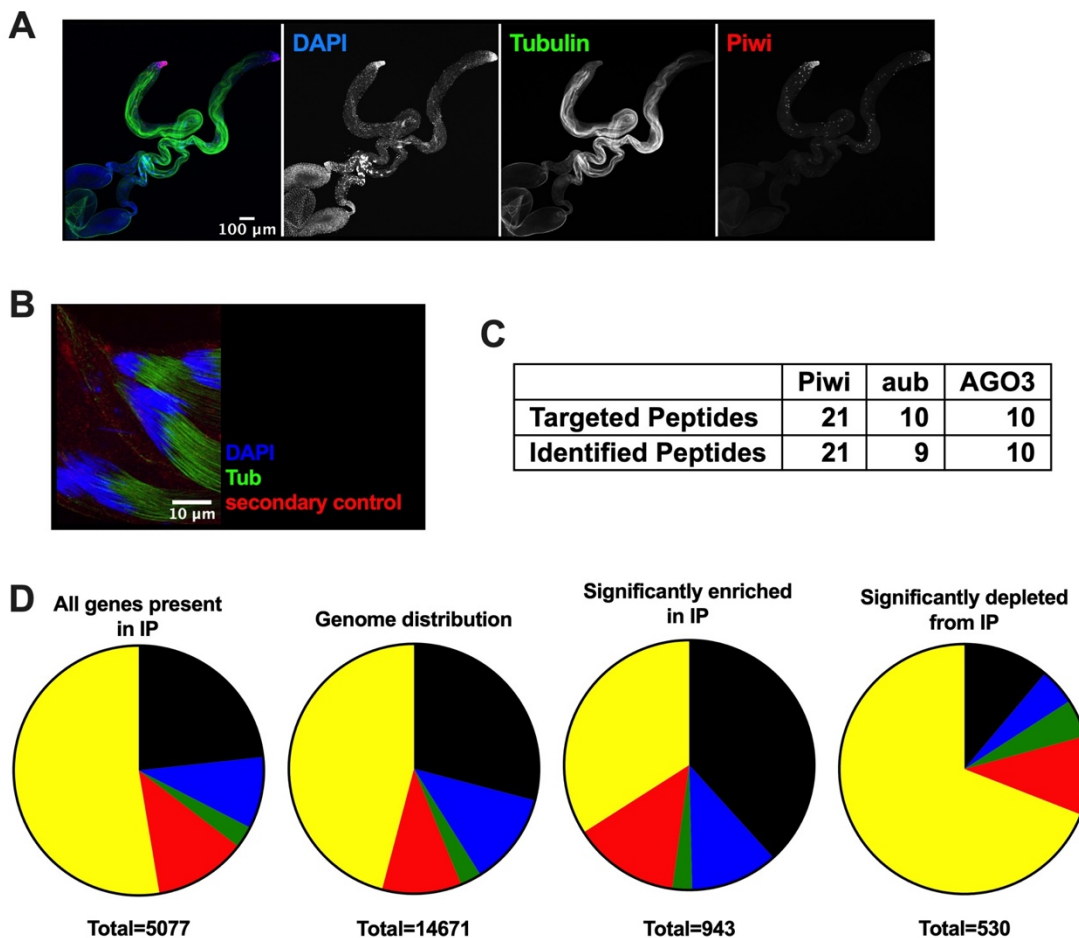
310 **Fig. 4:**



311
312 **Fig. 4: An intact piRNA-pathway is necessary for the intergenerational inheritance of a**
313 **physiological phenotype** A) crossing scheme for paternal diet-induced intergenerational
314 **metabolic reprogramming (IGMR); B) mRNA-seq of IGMR offspring embryos, Log₂FC control**
315 **vs paternal high-sugar for different Classes as introduced in Fig. 3 B (R = random gene set); C)**
316 **same as B but rank analysis instead of Log₂FC; D) rank analysis comparing mRNA-seq of IGMR**
317 **offspring embryos to paternal *aub^{Het}* offspring E) rank analysis comparing mRNA-seq of IGMR**
318 **offspring embryos to maternal *aub^{Het}* offspring, p value and pearson r are depicted in D and E; F)**
319 **whole body triglycerides of IGMR offspring as % of control-sugar matched value using wildtype**
320 **(WT) or PIWI pathway heterozygous mutant (*piwi*, *aub*) fathers n=12-25 individual triglyceride**
321 **assays of groups of 5 flies from at least 3 independent experiments; G) proposed model and**
322 **summary for the data presented**

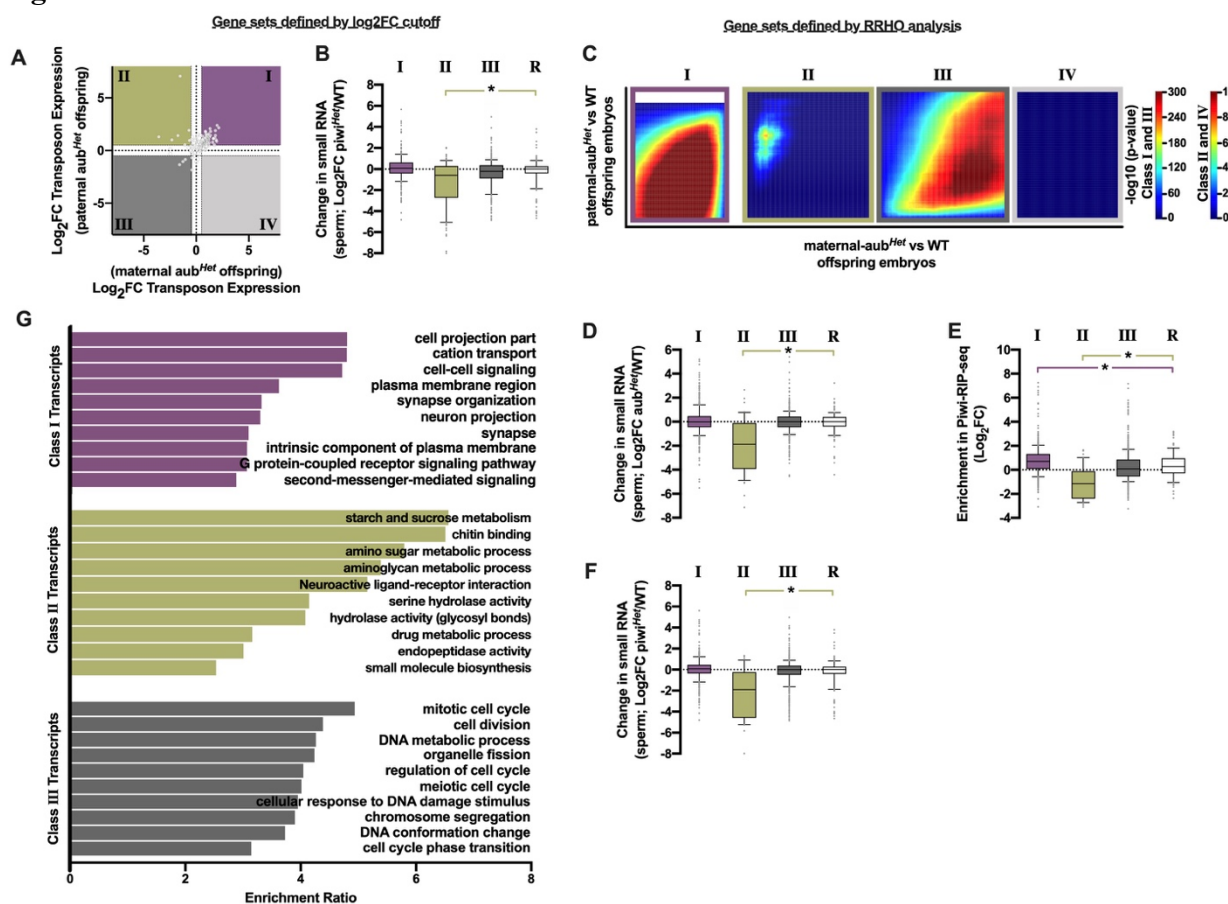
323
324

325 **Fig. S1:**



326
327 **Fig. S1: Presence of Piwi bound RNAs in mature sperm** A) immunofluorescence staining of
328 testis with Piwi (sc-390946) and tubulin antibodies; B) secondary antibody control staining for
329 Piwi (ab5207) staining in Fig. 2A; C) results of targeted mass spectrometry experiment identifying
330 peptides in isolated sperm; D) pie chart representation of chromatin state distribution of reads
331 mapping to features embedded in different chromatin states.

332 Fig.S2:

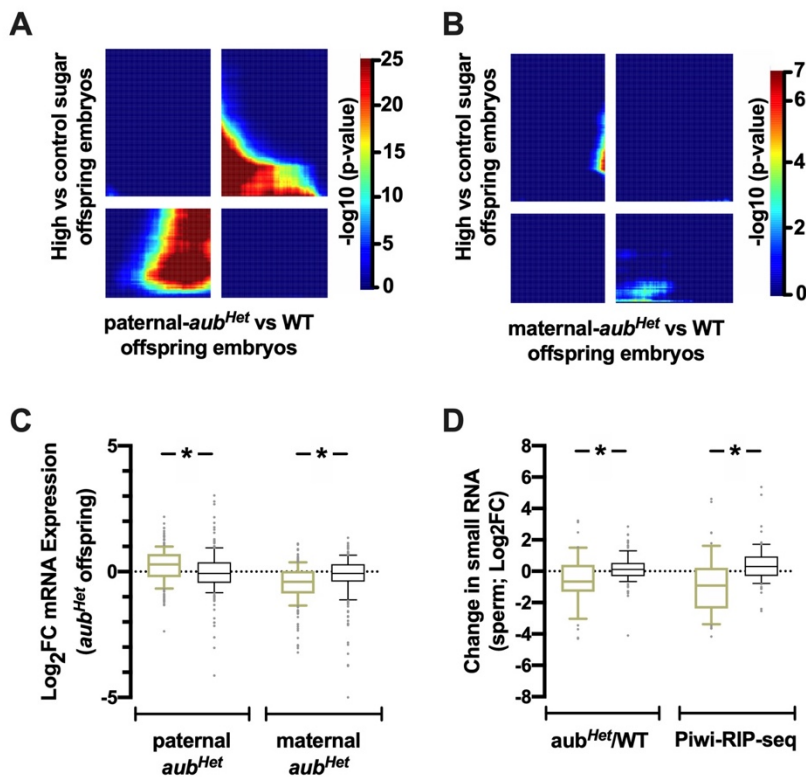


333
334

Fig. S2: Paternal piRNAs reprogram offspring

336 A) comparison of transposon expression changes induced by paternal and maternal *aub*^{*Het*}; B)
 337 Log₂FC of sperm sRNAs *piwi*^{*Het*}/WT, each boxplot represents genes present in a different
 338 quadrants (Class) from Fig. 3B, random gene set in white; C) Rank Rank Hypergeometric test of
 339 expression changes induced by paternal and maternal *aub*^{*Het*} confirms three Classes, different
 340 scales were applied to Class I/III and Class II/IV as depicted by the scale on the right; D) Log₂FC
 341 of sperm sRNAs *aub*^{*Het*}/WT, each boxplot represents genes present in a different quadrants from
 342 RRHO analysis in C, random gene set in white; E) Enrichment (Log₂FC IP/Input) in *piwi* pulldown
 343 experiment, each boxplot represents genes present in a different quadrants from RRHO analysis
 344 in C, random gene set in white; F) Log₂FC of sperm sRNAs *piwi*^{*Het*}/WT, each boxplot represents
 345 genes present in a different quadrants from RRHO analysis in C, random gene set in white; G)
 346 over representation analysis of different Classes depicted in Fig. 3B using WebGestalt on gene
 347 ontology terms included in Biological Processes noRedundant

348 **Fig. S3:**



349
350
351 **Fig. S3: An intact piRNA-pathway is necessary for the intergenerational inheritance of a**
352 **physiological phenotype.** Rank Rank Hypergeometric test of expression changes in embryos
353 induced by paternal diet intervention and A) paternal *aub*^{Het} B) maternal *aub*^{Het}; C) Log₂FC
354 mRNA expression changes of the 300 most upregulated genes in IGMR offspring in paternal
355 (green, left) and maternal (green, right) *aub*^{Het} offspring; D) Log₂FC changes of sperm sRNA
356 abundance in *aub*^{Het} sperm (green, left) and IP/Input (green, right), for those sRNAs mapping to
357 the 300 most upregulated genes in IGMR offspring random gene set in black.
358

359 **References and Notes:**

360 1 Czech, B. *et al.* piRNA-Guided Genome Defense: From Biogenesis to Silencing. *Annu
361 Rev Genet* **52**, 131-157, doi:10.1146/annurev-genet-120417-031441 (2018).

362 2 Ozata, D. M., Gainetdinov, I., Zoch, A., O'Carroll, D. & Zamore, P. D. PIWI-interacting
363 RNAs: small RNAs with big functions. *Nat Rev Genet* **20**, 89-108, doi:10.1038/s41576-
364 018-0073-3 (2019).

365 3 Siomi, M. C., Sato, K., Pezic, D. & Aravin, A. A. PIWI-interacting small RNAs: the
366 vanguard of genome defence. *Nat Rev Mol Cell Biol* **12**, 246-258, doi:10.1038/nrm3089
367 (2011).

368 4 Gainetdinov, I., Colpan, C., Arif, A., Cecchini, K. & Zamore, P. D. A Single Mechanism of
369 Biogenesis, Initiated and Directed by PIWI Proteins, Explains piRNA Production in Most
370 Animals. *Mol Cell* **71**, 775-790 e775, doi:10.1016/j.molcel.2018.08.007 (2018).

371 5 Aravin, A. A. *et al.* A piRNA-pathway primed by individual transposons is linked to de
372 novo DNA methylation in mice. *Mol Cell* **31**, 785-799, doi:10.1016/j.molcel.2008.09.003
373 (2008).

374 6 Robine, N. *et al.* A broadly conserved pathway generates 3'UTR-directed primary
375 piRNAs. *Curr Biol* **19**, 2066-2076, doi:10.1016/j.cub.2009.11.064 (2009).

376 7 Mohn, F., Handler, D. & Brennecke, J. Noncoding RNA. piRNA-guided slicing specifies
377 transcripts for Zucchini-dependent, phased piRNA biogenesis. *Science* **348**, 812-817,
378 doi:10.1126/science.aaa1039 (2015).

379 8 Ha, H. *et al.* A comprehensive analysis of piRNAs from adult human testis and their
380 relationship with genes and mobile elements. *BMC Genomics* **15**, 545,
381 doi:10.1186/1471-2164-15-545 (2014).

382 9 Yamtich, J., Heo, S. J., Dhahbi, J., Martin, D. I. & Boffelli, D. piRNA-like small RNAs
383 mark extended 3'UTRs present in germ and somatic cells. *BMC Genomics* **16**, 462,
384 doi:10.1186/s12864-015-1662-6 (2015).

385 10 Saito, K. *et al.* A regulatory circuit for piwi by the large Maf gene traffic jam in Drosophila.
386 *Nature* **461**, 1296-1299, doi:10.1038/nature08501 (2009).

387 11 Aravin, A. A. *et al.* Double-stranded RNA-mediated silencing of genomic tandem repeats
388 and transposable elements in the *D. melanogaster* germline. *Curr Biol* **11**, 1017-1027,
389 doi:10.1016/s0960-9822(01)00299-8 (2001).

390 12 Huang, X., Fejes Toth, K. & Aravin, A. A. piRNA Biogenesis in *Drosophila melanogaster*.
391 *Trends Genet* **33**, 882-894, doi:10.1016/j.tig.2017.09.002 (2017).

392 13 Ashe, A. *et al.* piRNAs can trigger a multigenerational epigenetic memory in the germline
393 of *C. elegans*. *Cell* **150**, 88-99, doi:10.1016/j.cell.2012.06.018 (2012).

394 14 Malone, C. D., Lehmann, R. & Teixeira, F. K. The cellular basis of hybrid dysgenesis and
395 Stellate regulation in *Drosophila*. *Curr Opin Genet Dev* **34**, 88-94,
396 doi:10.1016/j.gde.2015.09.003 (2015).

397 15 Papagiannouli, F. & Lohmann, I. Shaping the niche: lessons from the *Drosophila* testis
398 and other model systems. *Biotechnol J* **7**, 723-736, doi:10.1002/biot.201100352 (2012).

399 16 Sharma, U. *et al.* Small RNAs Are Trafficked from the Epididymis to Developing
400 Mammalian Sperm. *Dev Cell* **46**, 481-494 e486, doi:10.1016/j.devcel.2018.06.023
401 (2018).

402 17 Natt, D. *et al.* Human sperm displays rapid responses to diet. *PLoS Biol* **17**, e3000559,
403 doi:10.1371/journal.pbio.3000559 (2019).

404 18 Brennecke, J. *et al.* Discrete small RNA-generating loci as master regulators of
405 transposon activity in *Drosophila*. *Cell* **128**, 1089-1103, doi:10.1016/j.cell.2007.01.043
406 (2007).

407 19 Aravin, A. *et al.* A novel class of small RNAs bind to MILI protein in mouse testes. *Nature*
408 **442**, 203-207, doi:10.1038/nature04916 (2006).

409 20 Grivna, S. T., Beyret, E., Wang, Z. & Lin, H. A novel class of small RNAs in mouse
410 spermatogenic cells. *Genes Dev* **20**, 1709-1714, doi:10.1101/gad.1434406 (2006).

411 21 Lau, N. C. *et al.* Characterization of the piRNA complex from rat testes. *Science* **313**,
412 363-367, doi:10.1126/science.1130164 (2006).

413 22 Girard, A., Sachidanandam, R., Hannon, G. J. & Carmell, M. A. A germline-specific class
414 of small RNAs binds mammalian Piwi proteins. *Nature* **442**, 199-202,
415 doi:10.1038/nature04917 (2006).

416 23 Gonzalez, J., Qi, H., Liu, N. & Lin, H. Piwi Is a Key Regulator of Both Somatic and
417 Germline Stem Cells in the Drosophila Testis. *Cell Rep* **12**, 150-161,
418 doi:10.1016/j.celrep.2015.06.004 (2015).

419 24 Hutcheon, K. *et al.* Analysis of the small non-protein-coding RNA profile of mouse
420 spermatozoa reveals specific enrichment of piRNAs within mature spermatozoa. *RNA
421 Biol* **14**, 1776-1790, doi:10.1080/15476286.2017.1356569 (2017).

422 25 Filion, G. J. *et al.* Systematic protein location mapping reveals five principal chromatin
423 types in Drosophila cells. *Cell* **143**, 212-224, doi:10.1016/j.cell.2010.09.009 (2010).

424 26 Han, B. W., Wang, W., Li, C., Weng, Z. & Zamore, P. D. Noncoding RNA. piRNA-guided
425 transposon cleavage initiates Zucchini-dependent, phased piRNA production. *Science*
426 **348**, 817-821, doi:10.1126/science.aaa1264 (2015).

427 27 Senti, K. A., Jurczak, D., Sachidanandam, R. & Brennecke, J. piRNA-guided slicing of
428 transposon transcripts enforces their transcriptional silencing via specifying the nuclear
429 piRNA repertoire. *Genes Dev* **29**, 1747-1762, doi:10.1101/gad.267252.115 (2015).

430 28 Gu, T. & Elgin, S. C. Maternal depletion of Piwi, a component of the RNAi system,
431 impacts heterochromatin formation in Drosophila. *PLoS Genet* **9**, e1003780,
432 doi:10.1371/journal.pgen.1003780 (2013).

433 29 Cahill, K. M., Huo, Z., Tseng, G. C., Logan, R. W. & Seney, M. L. Improved identification
434 of concordant and discordant gene expression signatures using an updated rank-rank
435 hypergeometric overlap approach. *Sci Rep* **8**, 9588, doi:10.1038/s41598-018-27903-2
436 (2018).

437 30 Ost, A. *et al.* Paternal diet defines offspring chromatin state and intergenerational
438 obesity. *Cell* **159**, 1352-1364, doi:10.1016/j.cell.2014.11.005 (2014).

439 31 Liao, Y., Wang, J., Jaehnig, E. J., Shi, Z. & Zhang, B. WebGestalt 2019: gene set
440 analysis toolkit with revamped UIs and APIs. *Nucleic Acids Res* **47**, W199-W205,
441 doi:10.1093/nar/gkz401 (2019).

442 32 Piper, M. D. *et al.* A holidic medium for Drosophila melanogaster. *Nat Methods* **11**, 100-
443 105, doi:10.1038/nmeth.2731 (2014).

444 33 Raich, N., Contremoulin, V. & Karess, R. E. Immunostaining of Whole-Mount
445 Drosophila Testes for 3D Confocal Analysis of Large Spermatocytes. *J Vis Exp*,
446 doi:10.3791/61061 (2020).

447 34 Hayashi, R. *et al.* Genetic and mechanistic diversity of piRNA 3'-end formation. *Nature*
448 **539**, 588-592, doi:10.1038/nature20162 (2016).

449 35 Martin, M. Cutadapt removes adapter sequences from high-throughput sequencing
450 reads. *EMBnet.journal* **17**, 10-12, doi:DOI: <http://dx.doi.org/10.14806/ej.17.1.200> (2011).

451 36 Langmead, B. Aligning short sequencing reads with Bowtie. *Curr Protoc Bioinformatics
452 Chapter 11*, Unit 11 17, doi:10.1002/0471250953.bi1107s32 (2010).

453 37 Liao, Y., Smyth, G. K. & Shi, W. featureCounts: an efficient general purpose program for
454 assigning sequence reads to genomic features. *Bioinformatics* **30**, 923-930,
455 doi:10.1093/bioinformatics/btt656 (2014).

456 38 Robinson, M. D., McCarthy, D. J. & Smyth, G. K. edgeR: a Bioconductor package for
457 differential expression analysis of digital gene expression data. *Bioinformatics* **26**, 139-
458 140, doi:10.1093/bioinformatics/btp616 (2010).

459 39 Yu, G., Wang, L. G., Han, Y. & He, Q. Y. clusterProfiler: an R package for comparing
460 biological themes among gene clusters. *OMICS* **16**, 284-287,
461 doi:10.1089/omi.2011.0118 (2012).

462

463

464 **Author Contributions:**

465 A.L., A.Ö. and J.A.P. conceived, designed and supervised the study. A.L. and J.A.P wrote the
466 manuscript with feedback from all authors. A.L., L.E., A.G.M, O.L., M.S, U.K., M.I., L.Ö., M.G.L.R.,
467 E.B., performed fly work and dissections. U.K. perform library preparation for small RNA
468 sequencing. L.E. and M.I. optimized and performed piwi RIP-seq. A.L. performed
469 immunostaining. A.G.M. performed western blot analysis. T.R. prepared samples for mass
470 spec. E.B. performed embryo mRNA sequencing. E.C., I.B., D.N., A.L., D.P. performed
471 bioinformatic analysis. A.L. and T.V. supervised bioinformatic analysis.

472

473 **Funding sources:**

474 This work was supported by the Knut och Alice Wallenbergs Stiftelse [2015.0165]; Ragnar
475 Söderbergs stiftelse; Vetenskapsrådet [201503141]; European Research Council
476 [ERC-StG-281641].

477 **Supplementary Materials:**

478 Materials and Methods

479 Fly Food

480 Standard food: Agar 12 g/l, yeast 18 g/l, soy flour 10 g/l, yellow cornmeal 80 g/l, molasses 22 g/l,
481 malt extract 80 g/l, Nipagin 24 g/l, propionic acid 6,25 ml/l. Holidic diet was prepared according
482 to ³².

483

484 Fly stocks

485 w1118: used as WT stock

486 aub^{Qc42} – BDSC #4968: used for genetic crosses

487 piwi¹ – BDSC #43637: used for genetic crosses

488 T(2;3)TSTL, CyO: TM6B, Tb[1] – BDSC #42713: double balancer used for back-crossing

489

490 Fly Husbandry

491 Fly stocks were maintained on standard-diet at 25 °C on a 2-week generation cycle. To ensure a
492 common parental larva density and epigenetic background, 0-4 days old flies were manually sorted
493 to 15 males and 15 females per vial (or 45+45 in bottles) and allowed to lay eggs for 4 days. In
494 practice, flies were crossed on Thursday, flipped out on Monday and virgins collected the
495 following Monday. On Thursday flies were crossed again fulfilling a 2-week generation cycle.

496

497 Generation of flies for genetic crosses

498 To equalize the genetic background between mutant and WT strains we crossed the mutant lines
499 over double balancer lines so chromosomes can be followed using a visible marker. These flies
500 were then crossed to the WT strain and all chromosomes were replaced with WT chromosomes
501 except the one carrying the mutation and the respective balancer. Flies from the above cross were
502 crossed with WT and the resulting offspring without the balancer chromosome, was used for the
503 for the paternal and maternal mut^{Het} crosses.

504

505 Testis, sperm sack and ovary dissection

506 The reproductive tract of separated male and female flies was dissected in a drop of TC-100 insect
507 medium (Sigma) and connective tissue and other contaminating tissues were removed. Ovaries
508 were transferred to a tube containing insect medium. Testes with attached seminal vesicles (sperm
509 sacks) were transferred to a fresh drop of insect medium, where the sperm sack was separated from
510 the rest of the testis. Testes were further separated into three parts and transferred to different tubes
511 containing insect medium. Mature sperm was removed from the sperm sacks by puncturing them
512 and spooling the sperm onto clean forceps and transferred to a tube containing insect medium.
513 After a maximum of 30 min of dissection, collected tissues were snap frozen in liquid nitrogen.
514 When enough samples were collected the tissues were pelleted, the supernatant was discarded, and
515 the sperm pellet was re-suspended in 250µl of Trizol (Invitrogen).

516

517 Collection of staged *D. melanogaster* embryos

518 Virgin female flies were kept in egg-laying cages with apple-juice plates supplied with fresh yeast
519 paste for three days. Female virgin flies were crossed to male virgin flies in egg-laying cages at 25
520 °C in the morning and apple juice plates were changed approximately every 30 min until 2pm.
521 Subsequent apple juice plates were used for collection of embryos. To obtain stage 17 embryos
522 plates were left on the cage for 2 h and incubated for 16 h at 25 °C. Embryos on apple juice plates

523 were dechorionated using 50% PBS-TX (PBS-T containing 0.3 % Triton X-100) and 50 % bleach
524 for ~ 2 min. Dechorionated and detached embryos were collected and rinsed under a stream of
525 water. Embryos were then staged according to their morphology to maximize homogeneity in the
526 sample and immediately transferred to 250 μ l of Trizol solution for RNA isolation.

527

528 RNA isolation for sRNA-seq

529 Samples prepared in Linkoping: Frozen samples were homogenized in Qiazol with 0.15 g 0.2 mm
530 steel beads, Tissue Lyser 2 min 40 osc. RNA extraction was done using miRNeasy Micro kit
531 (Qiagen, Venlo, the Netherlands) and performed according to the manufacturer instructions, RNA
532 was eluted in 14 μ l of water and stored at -70 °C until library preparation.

533

534 Samples prepared in Freiburg: Dried RNA were shipped on dry ice and kept in -70 °C. Dried and
535 washed once with 80% ethanol and dried, dissolved in 20 μ l water, extraction was done using
536 miRNeasy Micro kit (Qiagen, Venlo, the Netherlands) and performed according to the
537 manufacturer instructions. RNA was eluted in 14 μ l of water and stored at -70 °C until library
538 preparation. Bioanalyzer confirmed the quality of the RNA.

539

540 Library preparation for sRNA-seq

541 Library preparation was done with NEBNext Small RNA Library Prep Set for Illumina (New
542 England Biolabs, Ipswich, MA) according to the manufacturer instructions with the following
543 minor customizations. All testicle samples, but not sperm samples, were downscaled to half
544 volume, using 3 μ l of input RNA instead of 6 μ l as recommended. In all steps the primers in the
545 kit were diluted 1:3 prior to use. 2S rRNA was blocked by adding anti-sense oligos (5'-TAC AAC
546 CCT CAA CCA TAT GTA GTC CAA GCA372 SpcC3 3'; 10 μ M) and set to hybridized in the
547 same step as NEBNext SR RT primer (pink). Amplification was made during 16 cycles and
548 amplified libraries were cleaned using Agencourt AMPure XP (Beckman Coulter, Brea, CA) and
549 size selected for 130 to 165 nt fragments on a pre-casted 6% polyacrylamide Novex TBE gel
550 (Invitrogen, Waltham, MA). Gel extraction was done using Gel breaker tubes (IST Engineering,
551 Milpitas, CA) in the buffer provided in the NEBNext kit. Disintegrated gels were incubated at 37
552 °C for 1 hour on a shaker, quickly frozen for 15 minutes at -80 °C, followed by another incubation
553 for 1 hour. Any remaining gel debris was removed by Spin-X 0.45 μ m centrifuge tubes (Corning
554 Inc., Corning, NY) as recommended by the NEBnext protocol. The libraries were precipitated
555 overnight at -80 °C by adding 1 μ l of GlycoBlue (Invitrogen) as co-precipitant, 0.1 times the
556 volume of Acetate 3M (pH 5.5), and 3 times the volume of 100% ethanol. Library concentrations
557 were estimated using QuantiFluor ONE ds DNA system on a Quantus fluorometer (Promega,
558 Madison, WI). Pooled libraries were sequenced on NextSeq 500 with NextSeq 500/550 High
559 Output Kit version 2, 75 cycles (Illumina, San Diego, CA). All pooled libraries passed Illumina's
560 default quality control.

561

562 Immunostaining

563 Immunostaining of whole mount testis and dissected sperm was carried out according to³³ in short:
564 testes were dissected in insect medium (Sigma, TC-100) and all incubation and washing steps were
565 carried out using home-made baskets in 96 well plates on an orbital shaker. Fixation was carried
566 out in 4% formaldehyde (methanol-free) in PBST (PBS and 0.2% Triton X-100) for 10 min at
567 room temperature. After three 5 min washing steps in PBST testes were permeabilized twice in
568 0.3% sodium-deoxycholate in PSTX for 30 min at room temperature. This was followed by three

569 5 min washing steps in PBSTX and 1h of blocking with 5% BSA in PBSTX at room temperature.
570 Primary antibody incubation (anti-Piwi antibody ab5207 - 1:500 dilution; anti-acetylated α -tubulin
571 (Lys40) antibody – 1:500, anti-Piwi antibody sc-390946 – 1:500 dilution) was carried out in
572 PBSTX+3% BSA at 4 °C overnight followed by one 20min wash with 300 mM NaCl in PBSTX
573 and three 5 min washes with PBSTX at room temperature. Secondary anti-Mouse Alexa Fluor 488
574 (1:1000; Molecular Probes) and anti-rabbit Alexa Fluor 555 (1:1000; Molecular Probes),
575 incubation lasted for 6h in PBSTX + 3% BSA at 4 °C samples were washed with 300 mM NaCl
576 in PBSTX for 20 min at room temperature, all steps were repeated for the second primary and
577 secondary antibodies and samples were mounted with Vectashield with DAPI (Vector Labs).
578 Confocal images were taken with a Zeiss LSM510 confocal scanning microscope with a C-
579 Apochromat \times 63, 1.4 NA oil immersion objective, using the diode 405 nm, the argon 488 nm, the
580 helium–neon 543 nm laser for excitation of DAPI, Alexa Fluor® -488, -555, respectively.
581

582 Triglyceride Determination

583 Groups of five flies (7-12 days old males) were crushed thoroughly in 100 μ l RIPA buffer,
584 sonicated and the homogenates were used for 96-well based colorimetric determination of
585 triglycerides (GPO Trinder, Sigma). Before absorbance measurement, plates were centrifuged, and
586 supernatants transferred to a new plate.
587

588 Mass Spectrometry (MS/MS) analysis

589 Sperm sack and pure sperm samples were analyzed by nanoLC-MS. Cells were lysed with lysis
590 Buffer (4% SDS, 100mM DTT, 50 mM Tris-HCl buffer pH 7.5, plus protease inhibitors (Roche)).
591 Then the extract was heated to 90°C for 3 min followed by residual chromatin shearing in
592 Bioruptor. Before MS-MS analysis samples were analyzed by SDS-PAGE followed by silver
593 staining (Thermofisher).
594

595 Western blotting

596 For protein extraction tissue were lysate adding 50 ml of Laemmli sample buffer 2x, heated at
597 95°C for 2 min and sheared in Biorupter (30sec/hard). Protein lysates were loaded on NUPAGE
598 4-12% precast gel (Life Technologies) in NUPAGE 1xMOPS buffer (Invitrogen). PageRuler Plus
599 Prestain Protein Ladder (Thermo Scientific) was used to indicate protein size. Proteins were
600 subsequently transferred to PVDF membranes. Before blocking, membranes were stained with
601 Ponceau solution (Sigma) and images were recorded. Membranes were blocked in phosphate
602 buffered saline plus 0,05% Tween 20 (PBST) and 5% BSA for 1 h at room temperature.
603 Membranes were incubated with primary Anti-Piwi antibody (ab5207) at 1:500 dilution overnight
604 at 4 °C, washed in PBST, and incubated with horseradish peroxidase (HRP) coupled secondary
605 antibodies (Anti-rabbit IgG, HRP-linked Antibody #7074) in the washing buffer with 1% skimmed
606 milk in PBST for 1 h at room temperature. Membranes were developed using SuperSignal™ West
607 Femto Maximum Sensitivity Substrate (Thermofisher).
608

609 Ribonucleoprotein Immunoprecipitation (RIP)

610 All steps were performed on ice or at 4 °C unless indicated otherwise. Samples with magnetic
611 beads were placed on magnetic rack for 30sec to ensure beads were pelleted. Dissected tissues
612 were thawed on ice and resuspended in PBS-T (0.05% Tween 20) supplemented with cOmplete,
613 mini EDTA-free protease inhibitor cocktail (Roche Diagnostics, GmbH, Germany) and RNase
614 inhibitor. Samples were transferred to a 60mm cell culture dish (on ice) and placed in a Bio-

615 LinkTMBLX 365 UV-crosslinker. Samples were crosslinked with UV light at 400 mJ/cm².
616 Samples were then transferred to a fresh 1.5 ml Eppendorf tube. 60 mm dish was then washed once
617 with 500 µl PBS-T and the wash was added to sample. Samples were then centrifuged 8000 x g at
618 4 °C for 5 min. Supernatant was carefully discarded and samples were resuspended in 250 µl-500
619 µl RIPA buffer (50mM Tris-HCl pH 7.5, 150 mM NaCl, 1% Triton-X 100, 0.1% SDS, 0.1% Na-
620 deoxycholate, 1mM EDTA, 1x cOmplete, mini EDTA-free protease inhibitor cocktail, RNase
621 inhibitor) and transferred to a Wheaton dounce tissue homogenizer chilled on ice. Samples were
622 homogenized 10x with a loose pestle and then 50x with a tight pestle to ensure complete tissue
623 homogenization. The homogenized samples were transferred to a fresh 1.5 ml Eppendorf tube and
624 kept on ice. The homogenizer was rinsed with 250 µl -500 µl IP dilution buffer (50 mM Tris-HCl
625 pH 7.5, 150 mM NaCl, 1x cOmplete, mini EDTA-free protease inhibitor cocktail, RNase inhibitor)
626 so as to dilute RIPA buffer 1:1 and the wash solution transferred to same tube as homogenized
627 sample. A 5% aliquot was taken of the lysate to be used as either input for IP-western blot
628 experiments or input for small RNA sequencing experiment. Sample stored at -20 °C.
629

630 Meanwhile, Diagenode CHiP-kit protein A magnetic beads were washed before use with 500ul
631 PBS-T and then 500 µl IP buffer (1:1 RIPA buffer and IP dilution buffer). Samples were pre-
632 cleared with pre-washed 25 µl Diagenode CHiP-kit protein A magnetic beads at 4 C with end-to-
633 end rotation for 2 hrs. A second batch of pre-washed Diagenode CHiP-kit protein A magnetic
634 beads were pre-loaded with rabbit-@-PIWI (ab5207) or IP control rabbit IgG: either 4 µg antibody
635 for 25 µl bead slurry for IP-Western blot experiments or with 8 µg antibody for 50 µl bead slurry
636 for IP-targeted proteomics experiment/smallRNA library preparation in 500 µl IP buffer (1:1 RIPA
637 buffer and IP dilution buffer). The bead/antibody solution was incubated at 4 °C for 4-6 hours
638 with end-to-end rotation. Pre-cleared samples were then pelleted on a magnetic rack and
639 supernatant transferred to the preloaded beads (following the disposal of the supernatant).
640 Antibody/preloaded beads/pre-cleared lysate mixture was incubated at 4 °C overnight with end-
641 to-end rotation. The following day, samples were washed 7 x 1 ml wash buffer (50 mM Tris-HCl
642 pH 7.5, 150 mM NaCl, 2 mM MgCl₂, 10% glycerol, 1% Empigen, RNase inhibitor)³⁴. Each wash
643 was carefully removed using vacuum suction. Samples used for IP-western blot or IP-targeted
644 proteomics experiments were eluted with 30 µl Bolt LDS sample buffer (Novex, Life
645 Technologies) supplemented with Bolt sample reducing agent (Novex, Life Technologies) at 95
646 °C, 1000 rpm for 5min then chilled on ice. Samples were stored at -20 °C until needed. If RNA
647 was needed following PIWI immunoprecipitation, beads were incubated with 100 µl TRI
648 Reagent® for 10 min at room temperature. Input samples were incubated with 10 volumes of TRI
649 Reagent® for 10 min at room temperature.
650

651 RNA isolation for small RNA library preparation

652 Tubes containing phase lock gel were prepared by the filling the lids of 0.2 ml PCR tubes with
653 phase lock gel. The tubes were then quickly spun down. Following incubation with TRI Reagent®,
654 the beads were pelleted using a magnetic rack and the supernatant was transferred to a tube
655 containing phase lock gel. Subsequently, 20 µl chloroform was added, the tubes mixed by shaking
656 and then centrifuged at 3100 x g for 10 min. The upper phase was transferred to a fresh tube
657 containing 50 µl isopropanol and 15 µg GlycoBlueTM, mixed by shaking and then incubated at -
658 20 °C overnight. The samples were then centrifuged at 3100 x g for 10min at 4 °C. The RNA pellet
659 was washed with 100 µl 75% ice cold ethanol, centrifuged at 3100 x g for 10min at 4 °C.
660 Supernatant was carefully decanted off samples and the pellet air dried. The pellet was then

661 resuspended in 4 μ l nuclease free water and stored at -80 $^{\circ}$ C. 5% of lysate used for PIWI IP (25
662 μ l out of 500 μ l lysate) was reserved to be used as input for small RNA sequencing experiment.
663 These samples were incubated with 250 μ l TRI Reagent[®] for 10min at room temperature.
664 Subsequently, 50 μ l chloroform was added, the tubes mixed by shaking and then centrifuged at
665 3100 x g for 10min. The upper phase was transferred to a fresh tube containing 125 μ l isopropanol
666 and 15 μ g GlycoBlueTM, mixed by shaking and then incubated at -20 $^{\circ}$ C overnight. The samples
667 were then centrifuged at 3100 x g for 10min at 4 $^{\circ}$ C. The RNA pellet was washed 1x with 250 μ l
668 75% ice cold ethanol, centrifuged at 3100 x g for 10min at 4 $^{\circ}$ C. Supernatant was carefully
669 decanted off samples and the pellet air dried. The pellet was then resuspended in 6.5 μ l nuclease
670 free water and stored at -80 $^{\circ}$ C.

671
672 IP and Input samples processed the same way from now on: The quality and concentration of the
673 RNA samples was analyzed by Agilent Small RNA kit on the Agilent 2100 Bioanalyzer system
674 and NanoDropTM. The RNA samples were then used to make small RNA libraries using the
675 NEBNext Small RNA Library Prep Kit for Illumina (E7330) according to the manufacturer's
676 instructions. Ligation of the 3'SR adapter was performed at 16 $^{\circ}$ C for 18 hrs. This longer
677 incubation at a reduced temperature increases ligation efficiency of methylated RNAs such as
678 piRNAs. Since *Drosophila* RNA is rich in 2S rRNA, a 2S blocking oligo was also used at a final
679 concentration of 0.1 μ M to exclude 2S RNA from any downstream reaction. 12 PCR cycles were
680 used to amplify the libraries.

681
682 QC and read mapping
683 Small RNA reads were trimmed for sequencing adapters using Trim Galore v0.5.0
684 (<https://github.com/FelixKrueger/TrimGalore>) in conjunction with Cutadapt v1.11³⁵. Low-quality
685 (Q<20) bases were also trimmed from the ends of reads, and reads were discarded if their length
686 was then less than 20 nucleotides following trimming.

687 Trimmed reads greater than 20 nucleotides in length were then mapped to dm6 genome (FlyBase
688 BDGP6.22 release) using the short-read aligner bowtie v1.2.3³⁶, allowing for one mismatch. If
689 there were multiple alignments, then only the highest quality alignment was retained (bowtie
690 options -M 1 --best --strata). Alignment files were sorted and indexed using SAMtools v1.8.

691
692 Hierarchical Feature Counting
693 Annotation data was downloaded from FlyBase, release BDGP6.22. The annotations were
694 stratified into 14 ordered feature categories: rRNA, tRNA, snRNA, snoRNA, pre miRNA, simple
695 repeats, complex repeats, Piwi RNA, 5' UTR, 3' UTR, protein coding exon, pseudogene, ncRNA,
696 and mitochondrial genome. The Piwi RNA cluster (n=114) annotations were from piPipes. Next,
697 using featureCounts (subread v2.0.0)³⁷, mapped reads were counted for each of the 13 categories
698 independently. A minimum overlap of 15 nucleotides was required, with the fractional counts
699 option was on. This counting was strand-specific and was done for both forward (sense) and
700 reverse (antisense) strands independently. Finally, using a custom script (<https://github.com/vari->
701 BBC/Piwi_RNA_pipeline), we did a hierarchical counting for the 13 categories. That is, for any
702 read annotated to multiple features, it was counted only for the feature highest in the category. So,
703 reads mapped to a Piwi RNA cluster within an exon were counted towards the Piwi RNA cluster
704 not the exonic feature. This approach assured that reads were assigned correctly, and ambiguities
705 from reads mapping to rRNA and other small RNA features were not included as Piwi RNAs. This
706 resulted in a counts file for sense and antisense features.

707

708 Differential Expression Analysis

709 The sense and antisense counts tables were imported into R v3.6.0. Features with counts of less
710 than 10 raw counts in less than 2 samples were removed. In addition, two complex repeat features
711 (LSU-rRNA_Dme and SSU-rRNA_Dme) were also removed. Following filtering, individual
712 contrasts for differential feature expression were done using edgeR v3.28.0³⁸. For all contrasts, a
713 general linear model was fit using appropriate covariates that varied depending on the contrast, but
714 included – where appropriate – treatment, tissue, knock, knock side, and genotype. Statistical
715 significance was assessed using a quasi-likelihood F test with multiple testing correction
716 performed with the Benjamini-Hochberg procedure.

717

718 GSEA

719 The genes comprising each biotype were used as gene sets to test for enrichment of certain biotypes
720 in certain phenotypes. Enrichment testing was done with GSEA as implemented in the
721 clusterProfiler v3.14.3 function ‘GSEA.’ Then thousand phenotype permutations were run³⁹. The
722 biotype annotation was from UCSC for dm6.

723

724 Overrepresentation Analysis (ORA)

725 ORA for RIP enriched transcripts was performed using WebGestalt³¹ with the following
726 parameters for the enrichment analysis: Minimum number of IDs in the category: 5; Maximum
727 number of IDs in the category: 500; FDR Method: BH; Significance Level: FDR < 0.05

728